Vaccine 37 (2019) 6112–6124

Contents lists available at ScienceDirect

Vaccine

journal homepage: www.elsevier.com/locate/vaccine

Respiratory syncytial virus prefusogenic fusion (F) protein nanoparticle vaccine: Structure, antigenic profile, immunogenicity, and protection

Nita Patel, Mike J. Massare, Jing-Hui Tian, Mimi Guebre-Xabier, Hanxin Lu, Haixia Zhou, Ernest Maynard, Daniel Scott, Larry Ellingsworth, Gregory Glenn, Gale Smith *

Novavax, Inc., Gaithersburg, MD, United States

ARTICLE INFO

Article history:
Received 22 December 2018
Received in revised form 6 July 2019
Accepted 26 July 2019
Available online 12 August 2019

Keywords:
Respiratory syncytial virus
Prefusogenic fusion glycoprotein
Vaccine
Cotton rat

ABSTRACT

Respiratory syncytial virus (RSV) is a major cause of severe respiratory disease in the very young, elderly, and immunocompromised for which there is no vaccine. The surface exposed RSV fusion (F) glycoprotein is required for membrane fusion and infection and is a desirable vaccine candidate. RSV F glycoprotein structure is dynamic and undergoes significant rearrangements during virus assembly, fusion, and infection. We have previously described an RSV fusion-inactive prefusogenic F with a mutation of one of two furin cleavage sites resulting in the p27 region on the N-terminus of F1 with a truncated fusion peptide covalently linked to F2. A processing intermediate RSV prefusogenic F has been reported in infected cells, purified F, budded virus, and elicited a strong immune response against p27 in RSV infected young children. In this report, we demonstrate that prefusogenic F, when expressed on the cell surface of Sf9 insect and human 293T cells, binds monoclonal antibodies (mAbs) that target prefusion-specific antigenic sites Ø and VIII, and mAbs targeting epitopes common to pre- and postfusion F sites II and IV. Purified prefusogenic F bound prefusion F specific mAbs to antigenic sites Ø and VIII and mAbs targeting pre- and postfusion sites II, IV, and p27. Mice immunized with prefusogenic F antigen produced significantly higher levels of anti-F IgG and RSV neutralizing antibodies than prefusion or postfusion F antigens and induced antibodies competitive with mAbs to sites Ø, VIII, II, and IV. RSV prefusogenic F neutralization antibody responses were enhanced with aluminum phosphate adjuvant and significantly higher than prefusion F. Prefusogenic F vaccine protected cotton rats against upper and lower respiratory tract infection by RSV/A. For the first time, we present the structure, antigenic profile, immunogenicity, and protective efficacy of RSV prefusogenic F nanoparticle vaccine.

1. Introduction

Human respiratory syncytial virus (RSV) is the cause of severe lower and upper respiratory tract infection (LRTI and URTI) for which an efficacious vaccine could have a significant public health benefit [1–3]. The fusion (F) glycoprotein is critical to the pathogenicity of the virus, takes on several forms from translation to infection, and is an attractive vaccine target. Studies with palivizumab (Synagis®), an approved monoclonal antibody (mAb) for prevention of severe RSV disease in high-risk newborns [4,5], and a follow-on product, motavizumab, present compelling evidence that neutralizing antibodies to F protein can protect against infection [6,7]. Multiple lines of evidence indicate that serum [8] and breast milk antibodies [9] to the RSV F glycoprotein are associated with reduced disease.

Human RSV is an enveloped virus in the *Pneumoviridae* family with two major subgroups: RSV/A and RSV/B, based on heterogeneity of the attachment (G) glycoprotein [10]. The fusion (F) protein serves a critical function in infectivity, and its sequence is conserved with ~90% homology between RSV/A and RSV/B subgroups with multiple shared antigenic sites [11]. The F protein is transcribed as a single inactive polypeptide (F0), which is cleaved by furin protease at two residues, 109 (site I) and 136 (site II), and removal of a 27-aa fragment (p27) generating covalently linked F2 and F1 subunits. Furin cleavage is required for membrane fusion activation [12]; however, the timing and cellular location of cleavage is not fully understood. Cleavage site II adjacent to the fusion domain in F1 is indispensable for fusion activation, whereas cleavage site I increases the efficiency of cleavage site II recognition [13]. Also, partially cleaved F protein intermediates have been reported in purified RSV virus [12]. In addition, a second intracellular furin cleavage of F can occur in human lung epithelial cells following macropinocytosis of RSV virus [14]. Ruiz-Alguello and

* Corresponding author.
E-mail address: gsmith@novavax.com (G. Smith).

https://doi.org/10.1016/j.vaccine.2019.07.089
0264-410X/

colleagues [13] reported that partially cleaved RSV F with a mutated furin site II resulted in a fusion-inactive protein highly resistant to thermal denaturation. Antigenic fingerprinting following primary RSV infection of young children identified an immunodominant epitope in p27 that declined with age [15]. Also, the removal of the N-glycosylation sequence in RSV F p27 resulted in enhanced antibody responses after DNA immunization [16]. These reports support a partially cleaved, prefusogenic F with p27 that is exposed on the surface of infected cells and virus membranes accessible to immune recognition, and thus physiologically relevant as a target vaccine candidate.

Fine structure mapping has identified the neutralizing epitope bound by palivizumab (site IIa) and the higher affinity motavizumab (site IIb) binding to F1 (residues 254–277) [17–19], as well as the non-neutralizing antibody 121I that binds site II at a position distinct from palivizumab or motavizumab [20]. Site IV is a neutralizing epitope on F1 that is the target of mAbs 101F and R1.42 [17,21,22]. Antigenic sites II and IV are conformation-independent and present on pre- and postfusion F conformations [23,24]. Antigenic site zero (Ø) is specific to the prefusion F structure, and the target of mAbs D25, AM22, AM14, and 5C4 [25–27]. Site Ø is a conformation-dependent site that includes F2 and F1 juxtaposed on prefusion F and disrupted by transition of RSV F from the pre- to the postfusion conformation [23,26]. Site VIII is a conformation-dependent site specific for prefusion F neutralizing antibodies. Monoclonal antibody hRSV90 heavy and light chains interact with amino acids within site Ø and near site II located on adjacent F-protomers [28].

In this report, the physical structure, antigenic profile, immunogenicity, and protection of RSV prefusogenic F [29] is compared to prefusion and postfusion F antigens. RSV prefusogenic F nanoparticle vaccine has been shown to be safe and immunogenic in healthy adults [30], women of childbearing age [31,32], older adults [33], and is currently in a global phase 3 trial in pregnant women as a maternal vaccine to protect newborns [NCT02624947].

2. Materials and methods

2.1. Expression and purification

Synthetic RSV F genes were cloned into pFasBacI (Invitrogen), downstream of the *AcMNPV* polyhedron promoter (GeneArt, Regensburg, DE, USA). *Spodoptera frugiperda* (Sf9) insect cells (Invitrogen, Grand Island, NY, USA) were maintained in serum-free medium as suspension cultures, and the recombinant baculovirus (BV) with the RSV F transgene were generated using the Bac-to-Bac BV [30]. The construction of a near full-length RSV F with a mutation of furin cleavage site proximal to the fusion domain KKQKQQ to KKRKRR and a 10 amino acid deletion of the fustion domain (Phe137–Val146) were described previously [29] and the sequence is available GenBank MN125707. For prefusogenic F (BV 1184) and prefusion F (BV 2145), BV-infected Sf9 cells were harvested by centrifugation and the cell pellets were extracted. Cell lysates were clarified and purified as previously described [29]. For postfusion F (BV 2128), BV-infected Sf9 cells were cultured for ~65 h at 27 °C, and supernatants were collected by centrifugation (4000g). Postfusion F (BV 2128) was purified with an immobilized metal affinity column (IMAC) and ion exchange chromatography. Purified RSV F proteins were concentrated to 205–443 μg mL^{-1} in formulation buffer.

2.2. SDS-PAGE analysis

Purified proteins were loaded onto 4–12% Bis-Tris NuPAGE gels with and without reduction per the manufacturer's instructions (Invitrogen, Thermo Fisher Scientific), and the gels were stained with Coomassie blue.

2.3. Analytical characterization of RSV F constructs

Sample preparation: Samples were concentrated to ~430 μg mL^{-1} for analysis. Prefusogenic F (BV 1184) was formulated in 22 mM sodium phosphate (pH 6.2), 150 mM NaCl, 1% histidine, and 0.032% w/v polysorbate 80 (PS80). Prefusion F (2145) and postfusion F (BV 2128) were formulated in 25 mM sodium phosphate (pH 6.8), 400 mM NaCl, and 0.05% w/v PS80.

Analytical ultracentrifugation (AUC): Sedimentation velocity experiments were conducted with a Beckman Coulter XL-I analytical ultracentrifuge at 20 °C. Samples were centrifuged at 25,000 rpm, with sedimentation data collected as radial intensity at a detection wavelength of 290 nm. Data were analyzed in UltraScan (AUC Solutions, LLC.) using two-dimensional spectrum analysis (2DSA), to obtain sedimentation coefficient (s20,W) distributions and calculate weighted average s20,W values. A partial specific volume of 0.8109 cm^3 g^{-1} was applied to all constructs.

Dynamic light scattering (DLS). A DynaPro PlateReader II instrument (Wyatt Technology Corp.) was used to determine the mean hydrodynamic diameter of the RSV F glycoproteins at 20 °C. Particle size distributions were determined by measuring the time-dependent intensity fluctuations of scattered laser light (819 nm wavelength, with a detection angle of 150°). The Z-average diameter (d.nm) was determined by the method of cumulants.

2.4. Cell surface expression of prefusogenic F, prefusion F, and full-length wild-type F glycoproteins by fluorescence-activated cell sorting (FACS) analysis

Sf9 infection. Sf9 cells were maintained in HyQ-SFX insect medium without serum (HyClone, Logan, UT, USA) at 27 ± 2 °C. Sf9 cells (2×10^6 cells mL^{-1}) were infected with a multiplicity of infection of 0.001 pfu/cell recombinant BV and cells harvested 44–48 h postinfection by centrifugation.

293T cell transfection. 293T cells were transfected with pcDNA 3580 encoding the prefusogenic F gene or pcDNA 3582 encoding the full-length wild-type RSV/A2 F0 gene each codon optimized for expression in human 293T cells and transfected using Lipofectamine 3000 (Invitrogen, Carlsbad, CA, USA) following the manufacturer's protocol.

FACS analysis. Sf9 and 293T cells were washed with 0.05% bovine serum albumin in PBS and incubated with 2.5 μg mL^{-1} of the indicated mAb for 30 min at 4 °C. After washing, cells were stained with allophycocyanin (APC) conjugated goat anti-mouse IgG (Jackson Immuno Research Laboratories, West Grove, PA, USA) or with phycoerythrin (PE) conjugated goat anti-human IgG (SouthernBiotech, Birmingham, AL, USA) at 4 °C for 30 min. The negative control cells were stained with APC or PE conjugated second antibody. For gating, positively stained cells were treated with palivizumab or with murine mAb 858-1 clone 1331H (EMD Millipore, Burlington, MA, USA).

2.5. Monoclonal antibody binding to RSV F proteins by bio-layer interferometry (BLI)

Antigenic site-specific mAb binding to RSV F prefusogenic, prefusion, and postfusion conformers was determined by BLI using an Octet OK384 instrument (Pall FortéBio, Menlo Park, CA, USA). Anti-human Fc BLI biosensor tips were used to immobilize mAbs D25 (site Ø), hRSV106 (site Ø), hRSV90 (site VIII), palivizumab (site II), RSHZ19 (site IV), and 121I (site VII). Anti-mouse Fc biosensor tips were used to immobilize R1.42.2 (site IV), R4.C6, a novel RSV neutralizing monoclonal antibody that binds to pre- and postfusion

F between sites II and IV (site II/IV; Novavax unpublished), and RSV7.10 (p27). Tips were exposed to mAbs (10 μg mL^{-1}) for ~600 s and equilibrated to baseline in equilibration buffer (Pall FortéBio) for 60 s. The coated tips were transferred to wells containing 20 μg mL^{-1} prefusogenic (BV 1184), postfusion (BV 2128), or prefusion (BV 2145) F and allowed to associate for 600 s followed by dissociation for 400 s. The percent antibody binding to the RSV F ligand was analyzed with Octet HT10.0 software (Pall FortéBio).

2.6. Competitive epitope binning by BLI

BLI epitope binning was used to evaluate the competitive interaction between site-specific mAbs bound to prefusogenic (BV 1184), prefusion (BV 2145), and postfusion (BV 2128) F proteins. After obtaining a baseline, RSV F ligands were immobilized onto activated amine-reactive (AR2G) biosensor tips (Pall FortéBio) for 600 s. Following blocking of nonspecific binding, tips were transferred to buffer for 60 s to establish a baseline then immersed in wells containing 100 μg mL^{-1} of the first antibody for 600 s, followed by immersion in wells containing 5 μg mL^{-1} of the competing second antibody for 400 s. The percent competition between the first and second antibody analyzed with Octet HT 10.0 software (Pall Forte Bio). Two mAbs were considered to be non-competing if binding of the second antibody was >40%. A level of 30–40% was judged to be intermediate or moderate competition, and <30% was considered strong competition.

2.7. Animal studies

Animal ethics statement. Mouse and cotton rat studies were conducted in compliance with the National Research Council Guide for the Care and Use of Laboratory Animals and the Animal Welfare Act Regulations. Cotton rats (*Sigmodon hispidus*) were sourced from Sigmovir Biosystems, Inc. (Rockville, MD, USA) and the study was conducted according to Sigmovir Biosystems' Institutional Animal Care and Use Committee (IACUC) approved protocol. The mouse study was conducted by Noble Life Sciences (Sykesville, MD, USA) in accordance with an IACUC approved protocol.

Mouse immunogenicity. The immunogenicity of the RSV F prefusogenic F was compared to prefusion F and postfusion F in mice. Age-matched female BALB/c mice were immunized by intramuscular (IM) injection in the thigh with 1.0 or 10 μg prefusogenic F (BV 1184), postfusion F (BV 2128), or prefusion F (BV 2145) adjuvanted with 30 μg aluminum phosphate (AdjuPhos®, Brenntag). Separate groups of mice were immunized with 10 μg of the RSV F antigens without adjuvant. Mice were immunized twice with the doses spaced 21 days apart. Serum was analyzed 2 weeks after the second immunization.

Cotton rat immunogenicity and RSV challenge. Age-matched (4–6 weeks old) female cotton rats were immunized by the IM route with two doses spaced 21 days apart. Animals (N = 6/group) were immunized with 1.0 μg of prefusogenic (BV 1184), prefusion (BV 2145), or postfusion (BV 2128) F antigens without or with 30 μg aluminum phosphate (AdjuPhos®, Brenntag). A placebo group was injected IM with 22 mM phosphate (pH 6.2), 150 mM NaCl, 1% histidine, and 0.03% PS80 formulation buffer. Serum was analyzed 21 days after the second immunization. Immediately following serum collection, immunized and placebo groups were intranasally (IN) challenged with 10^5 pfu RSV/A Long (Sigmovir Biosystems, Inc., Rockville, MD, USA).

2.8. Anti-RSV F IgG ELISA

Antibodies to prefusogenic, prefusion, and postfusion F were analyzed by ELISA as previously described [29,34]. Anti-RSV F IgG titers were reported at 50% of optical density as determined by a 4-parameter curve. For titers below the lower detection range, a titer of <1:100 (starting dilution) was assigned a value of 50, which was used to calculate the group geometric mean titer (GMT) and 95% confidence interval (CI).

2.9. Palivizumab competitive antibody (PCA) ELISA

Sera from cotton rats were analyzed for palivizumab competitive antibodies by ELISA as described [29,34]. PCA titers were converted to concentration of palivizumab in μg mL^{-1} by multiplying palivizumab titer by 2 as an experimentally derived conversion factor.

2.10. Specificity of RSV F antibodies produced by mice immunized with prefusogenic, prefusion, and postfusion F antigens by BLI

Sera from mice immunized with RSV F antigens were assessed for levels of antibodies competitive with antigenic site-specific mAbs by BLI. Ligand immobilized tips were dipped in wells containing diluted immune serum for 600 s and transferred to wells with 5 μg mL^{-1} of competing mAb D25 (site Ø), hRSV90 (site VIII), palivizumab (site II), R1.42 (site IV), or RSV7.10 (p27) for an additional 400 s. Competition between serum antibodies and mAb was analyzed with Octet HT 10.0 software. Competitive antibody equivalent (CAE) levels (μg mL^{-1}) were calculated based on the percent competition, the concentration of the competing antibody, and the serum dilution.

2.11. RSV/A micro-neutralization assay

Virus-neutralizing antibody titers were determined by inhibition of cytopathic effect (CPE) of RSV/A Long on HEp-2 cells [29]. Mouse and cotton rat sera were diluted, and an equal volume of 100 TCID50 of RSV/A Long was added to the wells. Cells were fixed and stained with 5% glutaraldehyde and 0.25% crystal violet. The limit of detection of the assay was 1:20, which was the lowest serum dilution in the assay.

2.12. Plaque assay

Virus load in the lung and nasal homogenates was determined with a quantitative plaque assay. Three weeks after the second immunization, cotton rats were challenged intranasally with 10^5 pfu RSV/A Long and sacrificed 4 days postinfection. Lung and nasal tissues were homogenized, and the homogenates were clarified by centrifugation and diluted. Confluent HEp-2 monolayers were infected in duplicate. Wells were overlaid, incubated, and cells were fixed and stained. Virus titers were expressed as pfu g^{-1} of lung or nasal tissue. GMTs and 95% CI were calculated with Prism Graph pad software (La Jolla CA, USA). The limit of detection of the assay was 200 pfu g^{-1} lung and 100 pfu g^{-1} nasal tissue.

2.13. Statistical methods

Anti-F IgG, PCA, CAE, virus neutralizing titers, and lung/nasal virus titers were plotted for individual animals, and the GMT and 95% CI determined for groups of mice (N = 10/group) or cotton rats (N = 6/group). Serum IgG titers and lung/nasal virus titers were $\log_{10}$ transformed, and the RSV/A neutralizing titers were $\log_2$ transformed to calculate significant differences between paired groups. *P*-values ≤ 0.05 were considered a statistically significant difference between two compared groups.

3. Results

3.1. RSV F glycoprotein constructs

RSV F constructs were synthetically produced from the RSV/A2 F0 gene sequence (Fig. 1A). Prefusogenic F (BV 1184) and prefusion F (BV 2145) glycoproteins were purified from Sf9 cell membranes following extraction with non-ionic detergent and postfusion F (BV2128) was secreted and purified by affinity chromatography from the culture supernatant. SDS-PAGE revealed that the purity of each of the antigens was >90% and had the expected F0, F1, F2, and single-chain F2-fp-F1 polypeptides under non-reduced and reduced conditions (Fig. 1B).

3.2. Biophysical characterization of RSV prefusogenic, prefusion, and postfusion F constructs

Prefusogenic F (BV 1184) migrated with a broad AUC sedimentation profile with a sedimentation coefficient of 23.3 S (f/f_0 = 1.11) and a mass of 1146 kDa. The prefusion F (BV 2145) sedimentation profile overlapped with the prefusogenic F profile. The sedimentation coefficient was 13.7 S (f/f_0 = 1.12), which was consistent with a smaller molecular mass of 710 kDa and an oligomeric particle consisting of 4 × F-trimers per particle. Postfusion F (BV2128) had a sedimentation coefficient of 5.0 S (f/f_0 = 1.12) and a narrow sedimentation profile representative of RSV F, primarily monomers and dimers (M_w = 123 kDa) (Fig. 2A and C).

Prefusogenic F had a particle size of 40 nm and PDI of 0.17 consistent with previous reports [29]. Prefusion F exhibited a smaller particle size of 23 nm and PDI of 0.15, and postfusion F appeared as similar size of 28 nm particle. Postfusion F had a highly variable PDI, which suggests the presence of larger aggregates that may bias the apparent size (Fig. 2B and C).

3.3. Cell surface expression of prefusogenic F

Fluorescence-activated cell sorting (FACS) analysis showed that Sf9 cells expressing RSV prefusogenic and prefusion F bound neutralizing antibodies targeting prefusion-specific sites Ø (D25) and VIII (hRSV90) as well as antibodies targeting neutralizing epitopes present on pre- and postfusion F, including sites II (palivizumab), IV (RSHZ19 and R1.42), and II/IV (R4.C6). Prefusogenic F was weakly bound by non-neutralizing site II mAb 121I (site VII), while the prefusion F failed to bind this antibody. Sf9 cells expressing prefusogenic F but not prefusion F were bound by mAb RSV7.10 (p27) (Fig. 3A).

Cell surface expression of prefusogenic F and wild-type (wt) RSV/A F0 on pcDNA transfected human 293T was also determined. Cells transfected with the prefusogenic F or wt-RSV/A F0 bound mAbs targeting sites Ø and VIII and mAbs targeting sites II, IV, II/IV, and, VII (Fig. 3B). Human 293T cells expressing prefusogenic F as expected were recognized by mAb RSV7.10 (p27). In addition, wt-RSV/A also bound p27 mAb but with lower intensity (Fig. 3B, bottom right panel), consistent with partial cleavage of F0 furin cleavage sites, thus retaining the p27 peptide linked to F2 or F1.

3.4. Site-specific mAb binding to RSV F conformers by BLI

BLI revealed that mAbs targeting the prefusion conformation-dependent sites Ø (D25 and hRSV106) and VIII (hRSV90) exhibited strong binding to prefusion F (>100%), intermediate binding to prefusogenic F (15–40%) and failed to bind the postfusion F conformer. The mAbs targeting sites II (palivizumab), IV (RSHZ19 and R1.42), and II/IV (R4.C6) exhibited strong binding to all RSV F conformers (>77%); mAb targeting p27 (RSV7.10) recognized only prefusogenic F, as p27 is not present on pre- or postfusion F (Figs. 4 and S1). These results indicate that key conformation-dependent prefusion F neutralizing epitopes and pre/postfusion neutralizing epitopes are stably expressed and accessible for antibody binding on purified prefusogenic F.

3.5. Competitive epitope binning of mAbs to RSV F conformers

The mAbs D25, hRSV106 (site Ø), and hRSV90 (site VIII) were used to map prefusion conformation-dependent epitopes. The mAbs palivizumab (site IIa), motavizumab and RSV3J20 (site IIb), RSHZ19 and R1.42 (site IV), and R4.C6 (II/IV) were used to map epitopes on both pre- and postfusion F. In addition, mAb RSV7.10 was used to map the RSV F p27 epitope. Prefusogenic F (BV 1184) was found to have a complex set of competitive binding interactions distinct from the prefusion or postfusion F conformers. Saturating mAb to site Ø blocked the binding of competing mAb to site IV and

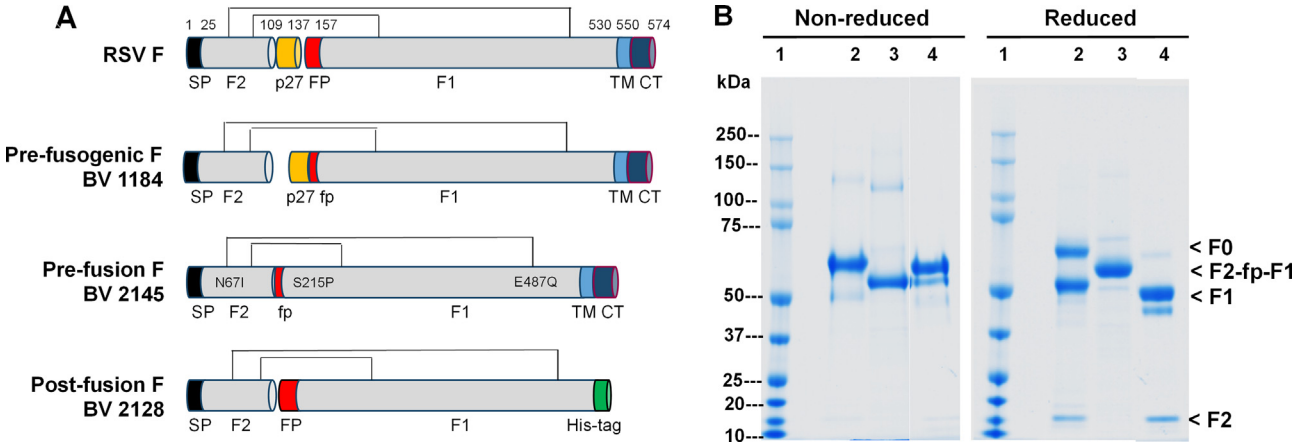

Fig. 1. RSV F glycoprotein constructs used in this study. (A) Linear diagram of RSV F glycoprotein constructs. Full-length wild-type RSV fusion glycoprotein showing the F1 and F2 ectodomain and the C-terminal transmembrane (TM, blue) and cytoplasmic tail (CT, purple). A cleavable signal peptide (SP, black) was added to the 5′ end of all constructs for expression in Sf9 insect cells. Prefusogenic F (BV 1184) construct was synthetically produced from the near full-length F protein with furin cleavage site II made protease resistant. The prefusion F construct (BV 2145) was generated from the full-length F protein with the transmembrane (TM) (blue) and cytoplasmic tail (CT) (purple). The postfusion F construct (BV 2128) was designed with the deletion of the TM/CT domains and an insertion of a C-terminal 6-his-tag (green). (B) Coomassie blue stained SDS-PAGE showing RSV F proteins non-reduced (left) and reduced (right): molecular weight standards (lane 1); prefusogenic F BV 1184 (lane 2); prefusion F BV 2145 (lane 3); and postfusion F BV 2128 (lane 4).

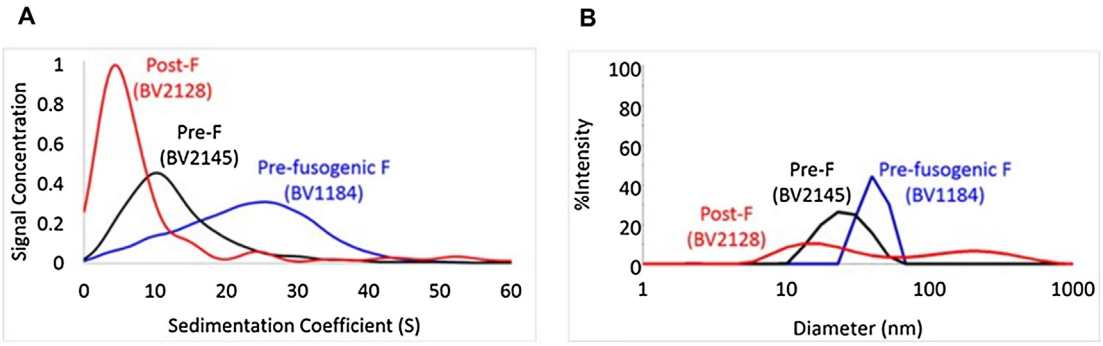

C

Hydrodynamic parameters of RSV F glycoprotein constructs

RSV F proteins	SV-AUC[1]			DLS[3]	
	$s^0_{20°C,w}$, Svedberg	M_w, app kDa[2]	f/f_0 $_{20°C,w}$	Z-average (nm)	PDI[4]
Prefusogenic F (BV 1184)	23.3 S	1,146	1.11	40	0.17
Prefusion F (BV 2145)	13.7 S	710	1.12	23	0.15
Postfusion F (BV 2128)	5.0 S	123	1.24	28	Multi-modal

[1] SV-AUC: Sedimentation velocity analytical ultracentrifugation data were collected at 20°C. Weight-averaged and water-adjusted sedimentation coefficients (*s20,W*) and frictional ratios (f/f_0) were obtained from fitting sedimentation velocity data to the adaptive space-time finite element solution of the Lamm equation using two-dimensional spectral analysis and applying a universally partial specific volume (V) of 0.8109 $cm^3\ g^{-1}$ to all constructs.
[2] M_w, app: Apparent molecular weights were calculated from the discrete species within the major peak of the sedimentation distribution.
[3] DLS: Dynamic light scattering data was collected at 20°C and processed by cumulant analysis.
[4] PDI: Polydispersity index.

Fig. 2. Hydrodynamic properties of RSV F prefusogenic, prefusion, and postfusion F proteins. (A) Sedimentation coefficient distributions of samples at 0.4 mg mL^{-1} centrifuged at 25,000–50,000 rpm. (B) Average particle size diameter (d.nm) and polydispersity index (PDI) of RSV F conformers determined by dynamic light scattering (DLS). (C) Apparent molecular mass determined from the sedimentation coefficient and particle size determined by DLS.

P27 but not site II, showing strong competition between site Ø, IV and P27. Binding of mAb to P27 site, completely blocked the binding of sites Ø and VIII but not site II, demonstrating strong competition between p27 mAb with prefusion-specific but not site II mAbs. Site IV did not block site II mAbs, showing no competition with site II. The binding of site Ø mAbs D25 and hRSV106 partially or completely competed the binding of mAbs targeting sites IV, II/IV, and P27. Similarly, site VIII mAb hRSV90 also partially or completely competed the binding of antibodies targeting sites IIa/b, IV, II/IV, and P27. Conversely, site IV mAbs strongly competed the binding of mAbs to sites Ø (D25, hRSV106) and VIII (hRSV90) on prefusogenic F (Fig. 5A). Prefusion-specific mAb D25 competed with hRSV106 (site Ø) and hRSV90 (site VIII). As previously established, palivizumab and motavizumab bound prefusion F (BV 2145) but did not compete binding of antibodies to site Ø or IV. Palivizumab and motavizumab partially competed binding of hRSV90 to site VIII, which was consistent with interaction of this antibody with amino acids within site Ø and near site II (Fig. 5B) [28]. The postfusion construct (BV 2128) efficiently binds antibodies targeting sites II, IV, and II/IV and not site Ø or VIII, consistent with BLI binding data presented here (Figs. 4 and 5C).

3.6. Immunogenicity of RSV F proteins in mice

The immunogenicity of RSV F conformers was compared in mice. All RSV F proteins elicited antibodies to the respective F-proteins. Anti-F IgG levels were significantly enhanced in animals immunized with the adjuvanted RSV F prefusogenic and prefusion but not postfusion antigens compared to the non-adjuvanted antigens ($P < 0.0001$). Adjuvanted prefusogenic F was more immunogenic than pre- or postfusion F antigens and produced significantly higher anti-F IgG titers ($P < 0.00001$). Anti-F IgG titers were 10- to 100-fold higher in animals immunized with prefusogenic F compared to prefusion F (Fig. 6A–C). RSV/A neutralizing antibody titers were also significantly enhanced in animals immunized with the adjuvanted prefusogenic F compared to mice immunized with adjuvanted pre- or postfusion F antigens ($P < 0.00001$) (Fig. 6D). Finally, anti-RSV F IgG responses correlated better to RSV neutralization titers in mice immunized with prefusogenic F vaccine compared to animals immunized with prefusion and postfusion F (Fig. 6E).

3.7. Specificity of antibodies produced by prefusogenic, prefusion, and postfusion F antigens

Mice immunized with prefusogenic F antigen had significantly higher levels of antibodies that compete the binding of mAbs targeting prefusion-specific sites Ø (D25) and VIII (hRSV90) compared to sera from mice immunized with prefusion or postfusion F antigens ($P < 6.5E-07$) (Fig. 7A and B). Animals immunized with prefusogenic F antigen also had significantly higher levels ($P < 2.7E-09$) of antibodies competitive with mAbs targeting sites II (palivizumab) and IV (R1.42) compared to antibody levels produced by prefusion or postfusion F antigens (Fig. 7C and D). In addition, mice immunized with prefusogenic F antigen also produced high levels (CAE = 350 μg mL^{-1}) of antibodies that competed R7.1 binding to p27 (Fig. 7E). Overall, prefusogenic F was significantly more immunogenic than the pre- or postfusion F antigens and produced high levels of antibodies to conformation-dependent prefusion-specific epitopes and those found on both pre- and postfusion F.

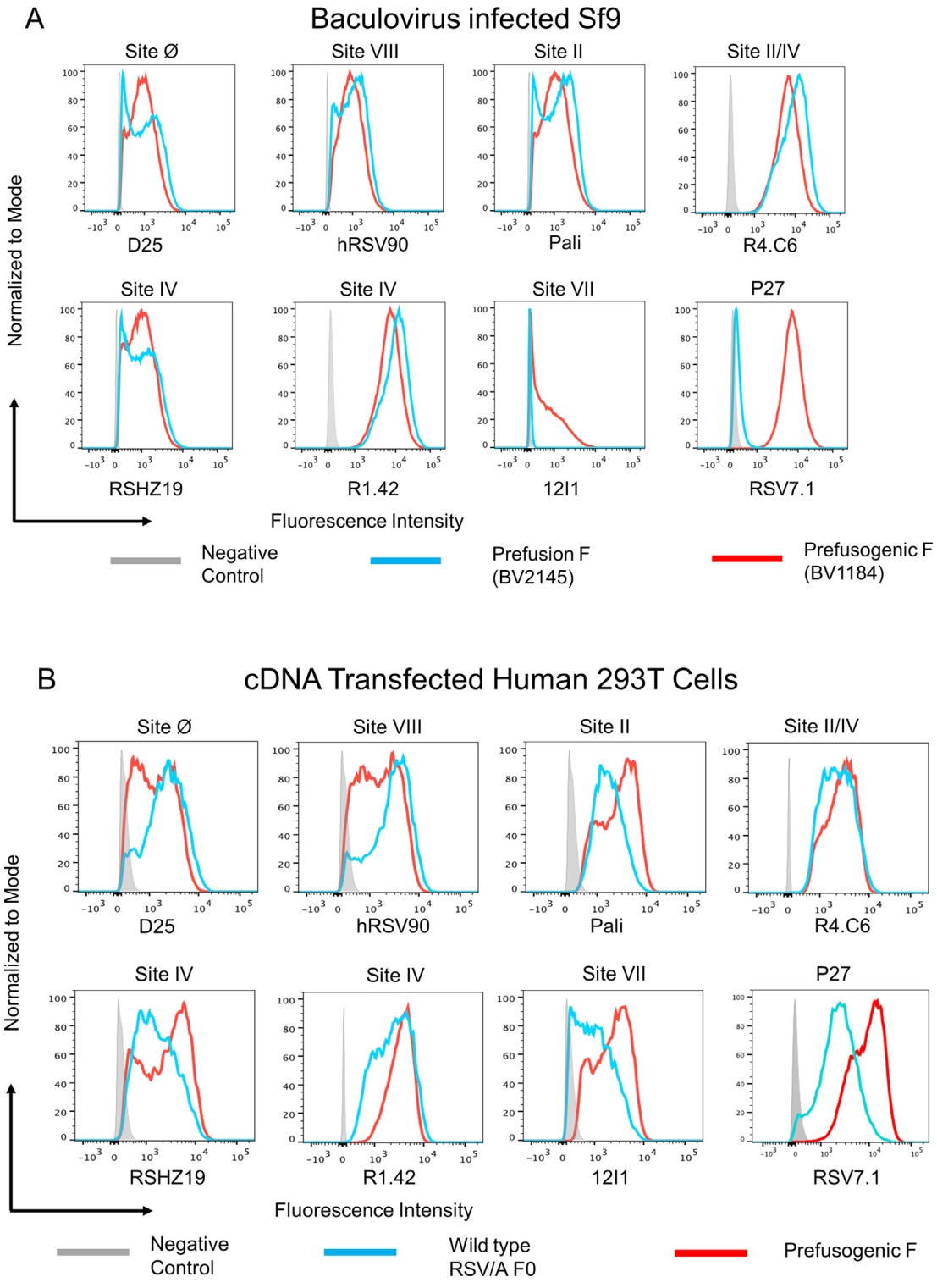

Fig. 3. FACS analysis of cell surface expressed RSV F prefusogenic F, prefusion F, and wild-type RSV F0 on Sf9 cells and transformed human 293T cells. (A) Sf9 cells were infected with recombinant prefusogenic F BV 1184 (red) or prefusion (blue). (B) Human 293T embryonic kidney cells were transfected with cDNA encoding prefusogenic F (red) or full-length wild-type RSV/A. Sf9 and 293T cells were harvested and treated with the indicated antigenic site-specific human or murine mAb. Infected and cDNA transfected cells were stained with phycoerythrin conjugated goat anti-human IgG or allophycocyanin conjugated goat anti-mouse. Palivizumab and murine mAb 858-1 clone 133-1H were used as positive controls for gating. Palivizumab (pali).

3.8. Immunogenicity and protective efficacy of RSV F antigens in cotton rats

Cotton rats are permissive to RSV URTI and LRTI and, therefore, are an established model for evaluation of the efficacy of RSV vaccines. Animals immunized with RSV F antigens with adjuvant had ~10-fold higher anti-RSV F IgG titers than did animals immunized without the adjuvant ($P \leq 0.02$) (Fig. 8A). PCA antigenic site II titers were significantly higher in animals immunized with prefusogenic ($P = 0.006$) and postfusion F ($P = 0.02$) antigens with adjuvant

Antigenic Site	Monoclonal Antibody	% Binding Monoclonal Antibody		
		Prefusogenic F	Prefusion F	Postfusion F
Site Ø	D25	40%	126%	0%
	hRSV106	15%	104%	0%
Site VIII	hRSV90	39%	149%	0%
Site II	Palivizumab	113%	126%	108%
Site IV	RSHZ19	104%	112%	107%
	R1.42	95%	89%	77%
Site II/IV	R4.C6	94%	85%	78%
P27	RSV.7.10	91%	0%	0%

No binding Intermediate binding Strong binding

Fig. 4. Bio-layer interferometry (BLI) of monoclonal antibody binding to RSV prefusogenic, prefusion, and postfusion F. BLI was used to measure the binding of RSV F site specific mAbs to purified prefusogenic, prefusion, and postfusion F. Octet HT10.0 software was used to calculate the percent binding, classified as strong (Orange), intermediate (Yellow), and no binding (White).

compared to animals immunized with antigens without adjuvant. Animals receiving prefusion F antigen had little or no measurable PCA titers (Fig. 8B). RSV/A neutralizing antibody levels were significantly higher in animals receiving RSV F antigens with adjuvant compared to those without adjuvant ($P < 0.01$). Furthermore, RSV/A neutralizing titers were significantly higher in animals receiving the prefusogenic F antigen with adjuvant compared to those without adjuvant ($P < 0.04$) (Fig. 8C).

Cotton rats were challenged intranasally to assess protection against RSV infection. Animals immunized with RSV F antigens had a significant reduction in virus load in the lungs compared to placebo-treated animals ($P \leq 0.001$). Lung homogenates from animals immunized with prefusogenic F antigen with or without adjuvant had little or no replicating virus. Animals receiving prefusion or postfusion F antigens with or without adjuvant also had significantly reduced virus load in the lungs compared to placebo-treated animals ($P \leq 0.001$). Virus loads were significantly reduced in animals immunized with RSV F antigens with adjuvant ($P \leq 0.03$) (Fig. 8D). Replicating virus loads in nasal samples were significantly reduced in animals immunized with the RSV F antigens (with or without adjuvant) compared to placebo ($P \leq 0.003$). Furthermore, animals immunized with RSV prefusogenic, prefusion, or postfusion F with adjuvant had significantly reduced nasal virus load compared to animals immunized without the adjuvant ($P \leq 0.02$) (Fig. 8E). Taken together, these results show that RSV prefusogenic F is significantly more immunogenic than prefusion F, and produced higher levels of anti-F IgG, PCA, and neutralizing antibodies than prefusion F, and provides similar protection from URTI and LRTI as prefusion F.

4. Discussion

Attempts to develop an RSV vaccine over the past 60 years have spawned corresponding applications of new tools to discern the critical attributes that are needed for an efficacious vaccine. Considerable emphasis has recently been placed on RSV F protein structures that reflect the prefusion crystal structure as providing a superior vaccine based on the presence of potent broadly neutralizing epitopes such as antigenic sites Ø and VIII [23,28]. It is less clear whether induction of immune responses to these epitopes will drive efficacy as it has yet to be seen whether prefusion-specific antibodies provide clinical protection against both RSV A and B viruses. On the other hand, high-affinity site II mAbs (palivizumab and motavizumab) have demonstrated clinical efficacy in pre-term and term infants via passive immunity in multiple randomized, placebo-controlled trials and are active against both RSV A and B strains [35,36]. Clinically, sero-epidemiology studies continue to implicate maternally derived, passively transfered anti-RSV F IgG as the immune measure associated with reduction of severe RSV disease in infants. Recently, investigators demonstrated that a 0.56 decrease in severity score in infants was observed for each 2-fold increase in anti-F IgG [37]. Together these studies indicate that induction of a high-titer anti-F IgG response composed of high-affinity antibodies that bind to conserved sites such as site II are important attributes of an immune response of a candidate vaccine. In previous clinical studies, we demonstrated that the RSV F nanoparticle vaccine induces high-titer anti-F IgG and high-affinity polyclonal site II binding antibodies [31,32].

The prefusion and postfusion F conforms have been extensively studied [24,38,39], but there is less information on the prefusogenic F structure. Complete furin cleavage of prefusogenic F conformation exposes the fusion peptide, and enables association with the target membrane [40]. The prefusogenic conformation contains the p27 fragment, which is absent in prefusion and postfusion F structures. We previously reported the generation of a prefusogenic F that retains the p27 region that assembles into nanoparticles comprised of multiple F-trimers [29].

In this study, we characterize particle structure, antigenic sites, immunogenicity, and protective efficacy of RSV prefusogenic F. Prefusogenic F had characteristics of both prefusion F and postfusion F, as it was bound by conformation-dependent mAbs that target prefusion F sites Ø and VIII, as well as mAbs that target antigenic sites II and IV common to both. As expected, mAb to the p27 peptide recognized only prefusogenic F and not prefusion F expressed on the surface of Sf9 cells. However, in human 293T cells, p27 mAb bound to the surface of cells expressing prefusogenic F and cells expressing wild type RSV/A2 F. This is evidence that the precursor RSV F0 was not fully processed when produced

A. Prefusogenic F

		Prefusion F			Prefusion F and Postfusion F						Prefusogenic F
		Ø		VIII	IIa	IIb		IV		II/IV	P27
1st	2nd mAb	D25	hRSV106	hRSV90	Pali	Mota	RSV3J20	R1.42	RSHZ19	4C6	RSV7.10
Ø	D25	0	57	50	42	50	41	23	32	23	25
	hRSV106	15	0	51	14	18	15	12	9	14	18
VIII	hRSV90	28	109	0	47	63	62	27	53	0	32
IIa	Pali	0	0	23	0	12	3	69	16	23	71
IIb	Mota	0	0	19	0	0	0	70	7	22	73
	RSV3J20	5	33	23	32	40	0	64	14	17	81
IV	R1.42	0	0	0	86	107	96	0	25	40	29
	RSHZ19	15	76	36	79	98	65	24	0	21	76
II/IV	R4.C6	0	0	0	26	32	31	33	22	0	85
P27	RSV.7.10	0	0	0	52	62	60	33	34	81	0

B. Prefusion F

		Prefusion F			Prefusion F and Postfusion F						Prefusogenic F
		Ø		VIII	IIa	IIb		IV		II/IV	P27
1st	2nd mAb	D25	hRSV106	hRSV90	Pali	Mota	RSV3J20	R1.42	RSHZ19	R4.C6	RSV7.10
Ø	D25	5	9	22	95	91	87	97	73	78	-
	hRSV106	10	8	81	75	87	81	76	71	69	-
VIII	hRSV90	0	107	4	2	20	67	78	75	5	-
IIa	Pali	95	75	38	4	13	10	86	72	5	-
IIb	Mota	97	77	54	0	2	2	83	75	0	-
	RSV3J20	96	71	84	1	6	4	87	80	2	-
IV	R1.42	84	80	84	83	89	86	0	0	75	-
	RSHZ19	88	79	89	87	108	90	8	1	80	-
II/IV	R4.C6	90	70	26	10	22	15	84	73	7	-
P27	RSV7.10	-	-	-	-	-	-	-	-	-	-

C. Postfusion F

		Prefusion F			Prefusion F and Postfusion F						Prefusogenic F
		Ø		VIII	IIa	IIb		IV		II/IV	P27
1st	2nd mAb	D25	hRSV106	hRSV90	Pali	Mota	RSV3J20	R1.42	RSHZ19	R4.C6	RSV7.10
Ø	D25	-	-	-	-	-	-	-	-	-	-
	hRSV106	-	-	-	-	-	-	-	-	-	-
VIII	hRSV90	-	-	-	-	-	-	-	-	-	-
IIa	Pali	-	-	-	0	9	11	74	57	6	-
IIb	Mota	-	-	-	0	0	4	73	59	2	-
	RSV3J20	-	-	-	3	7	0	67	42	6	-
IV	R1.42	-	-	-	21	26	16	0	0	2	-
	RSHZ19	-	-	-	32	44	42	26	0	15	-
II/IV	R4.C6	-	-	-	0	7	7	24	6	0	-
P27	RSV7.10	-	-	-	-	-	-	-	-	-	-

No Competition | Moderate Competion | Strong Competition | Self Binding

Fig. 5. Epitope binning of RSV F monoclonal antibodies with prefusogenic, prefusion, and postfusion F proteins. Antibody cross-competition was determined by BLI for prefusogenic F (A), prefusion F (B), and postfusion F (C) glycoproteins. Data indicate the percent binding of the competing second antibody in the presence of the first antibody. Dash (–) indicates antigenic sites are not present. Palivizumab (Pali) and Motavizumab (Mota). Binding of the second antibody >40% was non-competing (white), 30–40% was intermediate (gray), and <30% was strong competition (black). Yellow-colored cells indicate self-binding.

in human cells and consistent with a second furin cleavage leading to the transition from a prefusogenic to a metastable prefusion structure after internalization in a host cell [14]. It was previously suggested that partially cleaved intermediate RSV F protomers may be in the same oligomers with fully active prefusion F [13]. In addition, prefusogenic intermediates are found not only in purified F protein, but also in purified virus [12].

The prefusogenic F nanoparticle vaccine was highly immunogenic and produced significantly greater levels of virus-neutralizing antibodies than pre- or postfusion F antigens in immunized mice. Prefusogenic F also induced significantly higher levels of polyclonal antibody competitive with mAb binding to sites Ø (D25), VIII (hRSV90), and statistically greater competitive responses against monoclonal antibodies to sites II (palivizumab) and IV (R1.42). These results confirmed that key neutralizing antigenic sites are represented on the prefusogenic F antigen and are readily recognized by the immune system. Antibody competitive with RSV F sites II and IV also were significantly increased in immune sera from RSV prefusogenic compared to prefusion F immunized animals. A recent report describing the transient opening and dissociation of full-length RSV F trimers on the surface of cells suggests modifications like adding of disulfide bridges to stabilize prefusion F may restrict trimer mobility and epitope recognition [42]. Thus, the significantly higher responses to RSV F

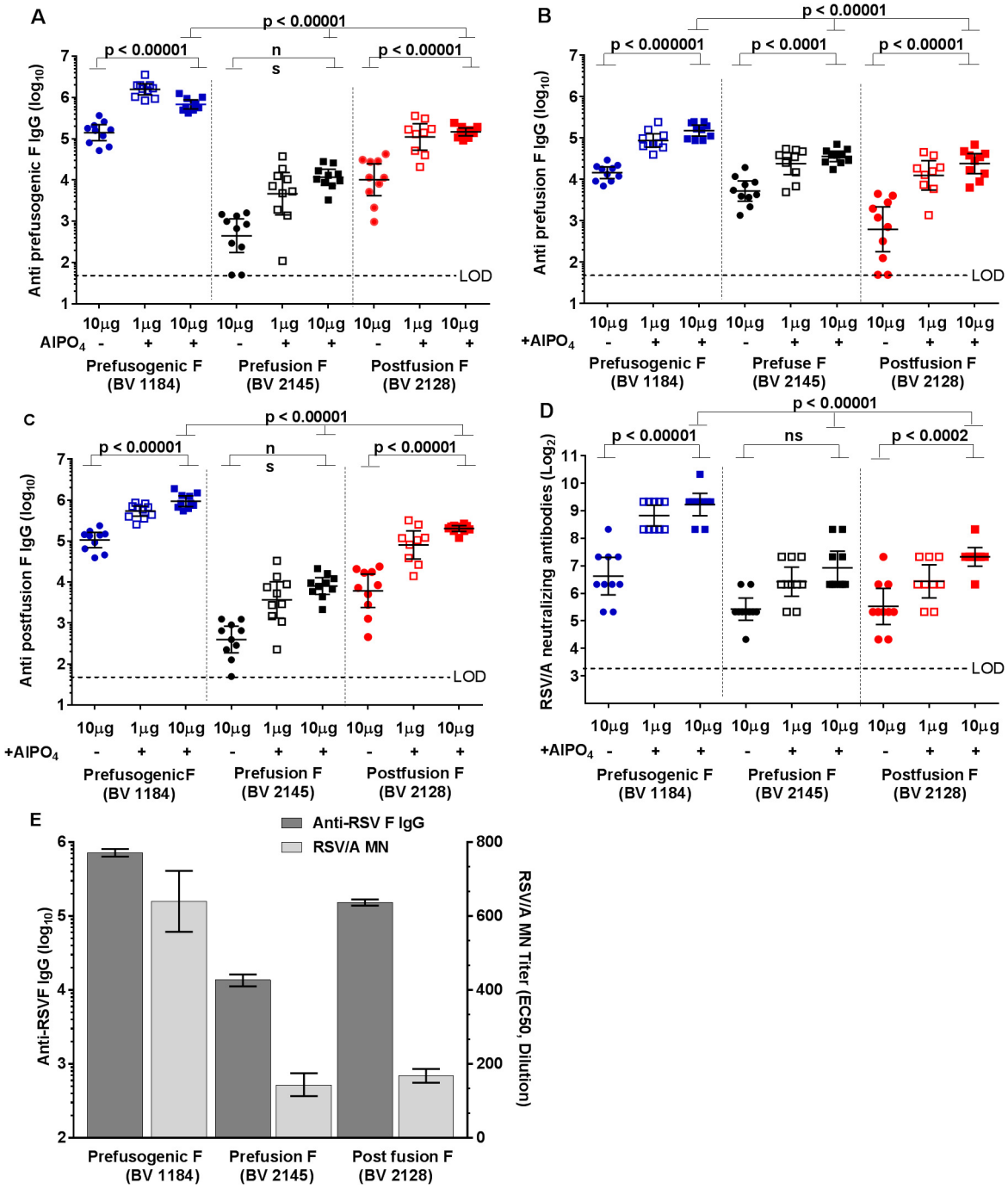

Fig. 6. Immunogenicity of RSV F glycoprotein antigens in mice. Serum from immunized mice was analyzed for (A) anti-prefusogenic F IgG, (B) anti-prefusion F IgG, (C) anti-postfusion F IgG titers, and (D) RSV/A neutralizing antibody titers. (E) Anti-RSV F IgG titers compared to RSV/A2 neutralizing antibody titers. The horizontal bars indicate the group geometric mean titer (GMT) and the error bars indicate the 95% CI (N = 10/group). The horizontal dashed line indicates the limit of detection (LOD) for each assay. Statistical significance between paired groups is indicated. Not significant (ns).

antigenic sites II and IV and superior immunogenicity and protective efficacy of prefusogenic RSV F vaccine may in part be due to the absence of mutations like in prefusion F constructs that may restrict protein mobility and thus recognition of B-cell receptors. In a second animal model, cotton rats immunized with prefusogenic F antigen with adjuvant produced significantly higher levels of functional neutralizing antibodies than did animals immunized with prefusion F. Cotton rats immunized with prefusogenic, prefusion, and postfusion F antigens were completely protected against LRTI and partially protected against URTI with RSV/A.

In this report, we characterize an RSV F nanoparticle vaccine based on a near full length, incompletely furin-cleaved, membrane-associated heterodimer trimers that form non-aggregated 40 nm protein – PS80 detergent particles with an average of six trimers per particle. A prefusion F formed 23 nm nanoparticles with an average of four trimers per particle. In contrast, a C-terminal truncated, secreted RSV postfusion F formed a mixture of monomers and higher-order oligomers that were aggregated. Previous studies indicated that RSV F vaccine formed discrete nanoparticles, derived from multiple F trimers [29]. This

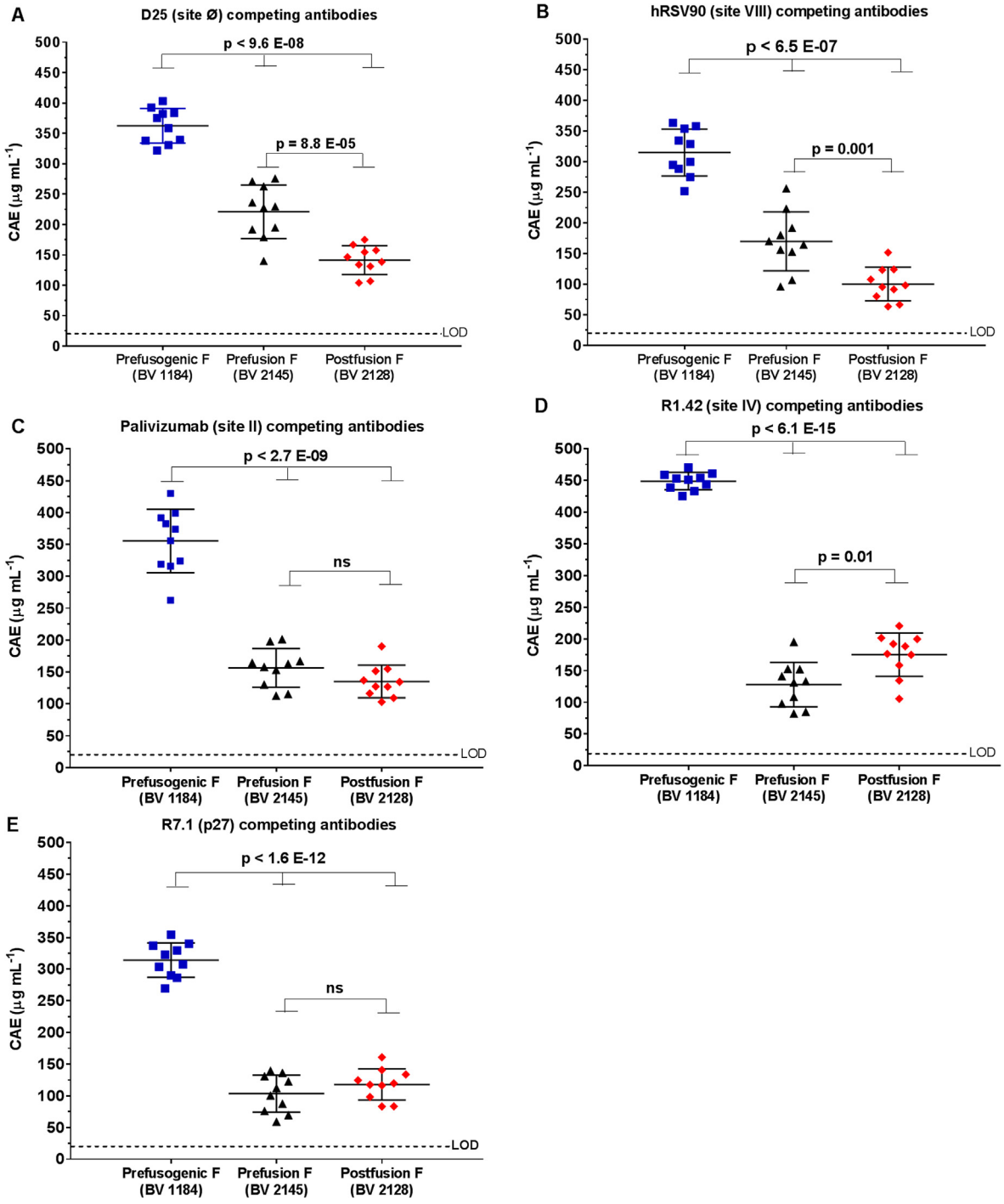

Fig. 7. Specificity of RSV F antibodies produced by immunizing mice with prefusogenic, prefusion, and postfusion F antigens. The specificity of antibodies elicited by immunizing with RSV F antigens was determined by competitive antibody binding of immune serum with site-specific mAbs by BLI. Horizontal bars indicate the group geometric mean, the error bars indicate the 95% CI (N = 10/group), and dashed lines indicate the limit of detection (LOD). Statistical significance between paired groups is indicated. Not significant (ns).

was confirmed in the current study using RSV prefusogenic F drug substance from a GMP manufacturing lot that formed 40 nm particles with low polydispersity, and was not aggregated. Based on relatively low-resolution electron microscopy and two-dimensional class averaging images, it was suggested that the RSV prefusogenic F vaccine structure was consistent with a postfusion conformation [29]. However, the antigenic characterization provided here and a recent report of RSV prefusogenic F vaccine protection of palivizumab-resistant mutant virus [41] indicate that epitopes associated with the prefusion form of F are present. In addition, the presence of p27 is consistent with observations that p27 is associated with a prefusogenic form of RSV F, upstream of the formation of a metastable prefusion, and absent for postfusion F.

This is the first study to compare the structure, antigenic profile, immunogenicity, and protective efficacy of three conformational structures of the RSV F glycoprotein. The RSV prefusogenic F was

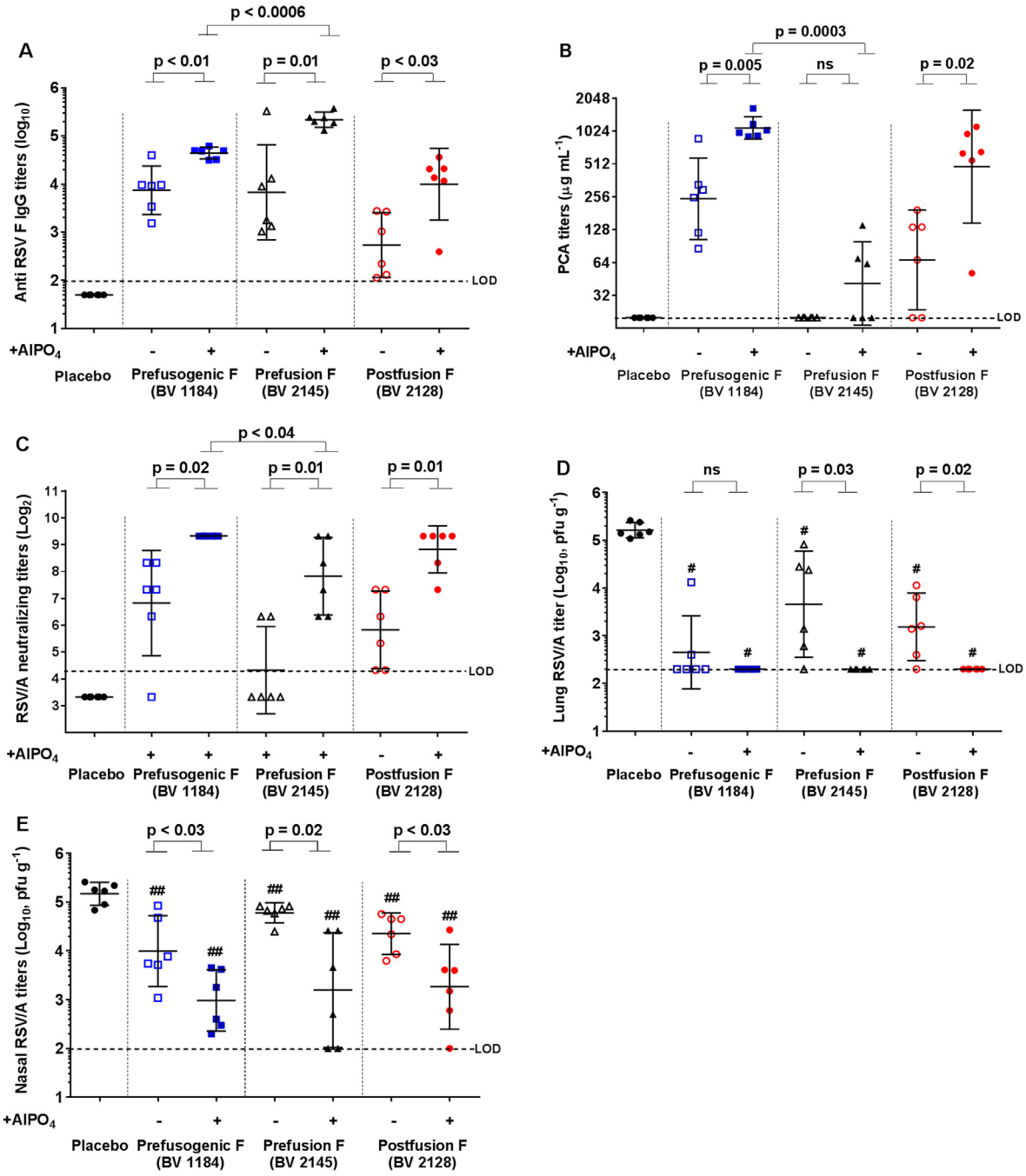

Fig. 8. Immunogenicity and protective efficacy of RSV F antigens cotton rats. Cotton rats were immunized with prefusogenic F (BV 1184), postfusion F (BV 2128), or prefusion F (BV 2145). The placebo group received formulation buffer. (A) Anti-RSV F IgG titers. (B) Palivizumab competitive antibody (PCA). (C) RSV/A neutralizing antibody titers. Lung (D) and nasal (E) homogenates were analyzed for replicating virus by a quantitative plaque assay. The vertical bars indicate the group GMT and the error bars indicate the 95% CI (N = 6/group). The vertical dashed lines indicate the limit of detection (LOD) for each assay. # indicates significant difference ($P \leq 0.001$) in virus load in lung homogenates of vaccinated animals compared to the placebo group. ## indicates significant difference ($P \leq 0.003$) in virus load in the nasal homogenates of vaccinated animals compared to the placebo group. Statistical significance between paired groups is indicated.

shown to present key virus neutralizing epitopes present on RSV F prefusion and postfusion structures. Sera from animals immunized with prefusogenic F had high levels of antibodies that compete for binding with mAbs that target key neutralizing epitopes. The induction of polyclonal antibodies that recognize a wide range of RSV neutralizing epitopes may lead to an efficacious vaccine, and clinical evaluation of an RSV prefusogenic F vaccine is underway.

Authors contributions

Authors NP, MJM, JHT, MGX, HL, HZ, EM, and DS contributed to conceptualization of experiments, generation of data and analysis, and interpretation of the data. Authors GS, GG, and LE contributed to drafting, making critical revisions, and giving approval for submission.

Funding

Support of this work was provided by Novavax, Inc. The funder had no role in the study design, data collection and analysis, decision to publish, or preparation of the manuscript.

Declaration of Competing Interest

Authors NP, MJM, JHT, MGX, HL, HZ, EM, DS, LE, GG, and GS are current or past employees of Novavax, Inc., a for-profit organization, and these authors own stock or hold stock options. These authors have submitted and have pending patent applications related to the work. These interests do not alter the authors' adherence to policies on sharing data and materials.

Acknowledgments

The authors were responsible for all content and editorial decisions, and received no honoraria related to the development of this manuscript. All authors contributed to the research, writing, and reviewing of all drafts of this manuscript and approved the final version. Editorial support in the preparation of this manuscript was provided by Phase Five Communications, funded by Novavax, Inc.

Data availability

All relevant data are within the manuscript and the associated supporting information files.

Appendix A. Supplementary material

The following is available online at www.mdpi.com/xxx/s1, Fig. S1. RSV F specific monoclonal antibody binding to different conformational structures of F glycoprotein. Additional information on materials and methods are included in the Supplementary Materials. Supplementary data to this article can be found online at https://doi.org/10.1016/j.vaccine.2019.07.089.

References

[1] Kim HW, Canchola JG, Brandt CD, Pyles G, Chanock RM, Jensen K, et al. Respiratory syncytial virus disease in infants despite prior administration of antigenic inactivated vaccine. Am J Epidemiol 1969;89:422–34. https://doi.org/10.1093/oxfordjournals.aje.a120955.

[2] Piedimonte G, Perez MK. Respiratory syncytial virus infection and bronchiolitis. Pediatr Rev 2014;35:519–30. https://doi.org/10.1542/pir.35-12-519.

[3] Mazur NI, Higgins D, Nunes MC, Melero JA, Langedijk AC, Horsley N, et al. The respiratory syncytial virus vaccine landscape: lessons from the graveyard and promising candidates. Lancet Infect Dis 2018;18:e295–311. https://doi.org/10.1016/S1473-3099(18)30292-5.

[4] The IMpact-RSV Study Group. Palivizumab, a humanized respiratory syncytial virus monoclonal antibody, reduces hospitalization from respiratory syncytial virus infection in high-risk infants. Pediatrics 1998;102(Pt 1):531–7. https://doi.org/10.1542/peds.102.3.531.

[5] American Academy of Pediatrics Committee on Infectious Diseases, American Academy of Pediatrics Bronchiolitis Guidelines Committee. Updated guidance for palivizumab prophylaxis among infants and young children at increased risk of hospitalization for respiratory syncytial virus infection. Pediatrics 2014;134:415–20. https://doi.org/10.1542/peds.2014-1665.

[6] Sandritter T. Palivizumab for respiratory syncytail virus prophylaxis. J Pediatr Health Care 1999;13:191–5. https://doi.org/10.1016/S0891-5245(99)90039-1.

[7] Huang K, Incognito L, Cheng X, Ulbrandt ND, Wu H. Respiratory syncytial virus-neutralizing monoclonal antibodies motavizumab and palivizumab inhibit fusion. J Virol 2010;84:8132–40. https://doi.org/10.1128/JVI.02699-09.

[8] Kulkarni PS, Hurwitz JL, Simões EAF, Piedra PA. Establishing correlates of protection for vaccine development: considerations for the respiratory syncytial virus vaccine field. Viral Immunol 2018;31:195–203. https://doi.org/10.1089/vim.2017.0147.

[9] Mazur NI, Horsley N, Englund JA, Nederend M, Magaret A, Kumar A, et al. Breast milk prefusion F IgG as a correlate of protection against respiratory syncytial virus acute respiratory illness. J Infect Dis 2018. https://doi.org/10.1093/infdis/jiy477.

[10] Mufson MA, Orvell C, Rafnar B, Norrby E. Two distinct subtypes of human respiratory syncytial virus. J Gen Virol 1985;66(Pt 10):2111–24. https://doi.org/10.1099/0022-1317-66-10-2111.

[11] Tapia LI, Shaw CA, Aideyan LO, Jewell AM, Dawson BC, Haq TR, et al. Gene sequence variability of the three surface proteins of human respiratory syncytial virus (HRSV) in Texas. PLoS ONE 2014;9:e90786. https://doi.org/10.1371/journal.pone.0090786.

[12] González-Reyes L, Ruiz-Argüello MB, García-Barreno B, Calder L, López JA, Albar JP, et al. Cleavage of the human respiratory syncytial virus fusion protein at two distinct sites is required for activation of membrane fusion. Proc Natl Acad Sci U S A 2001;14(98):9859–64. doi: 10.1073.pnas.151098198.

[13] Ruiz-Arguello M, Martin D, Wharton S, Calder L, Martin SR, Cano O, et al. Thermostability of the human respiratory syncytial virus fusion protein before and after activation: implications for the membrane-fusion mechanism. J Gen Virol 2004;85(Pt 12):3677–87. https://doi.org/10.1099/vir.0.80318-0.

[14] Krzyzaniak MA, Zumstein MT, Gerez JA, Picotti P, Helenius A. Host cell entry of respiratory syncytial virus involves macropinocytosis followed by proteolytic activation of the F protein. PLoS Pathog 2013;9:e1003309. https://doi.org/10.1371/journal.ppat.1003309.

[15] Fuentes S, Coyle EM, Beeler J, Golding H, Khurana S. Antigenic fingerprinting following primary RSV infection in young children identifies novel antigenic sites and reveals unlinked evolution of human antibody repertoires to fusion and attachment glycoproteins. PLOS Pathog 2016;12:e1005554. https://doi.org/10.1371/journal.ppat.1005554.

[16] Leemans A, Boeren M, Van der Gucht W, Pintelon I, Roose K, Schepens B, et al. Removal of the N-glycosyalion sequon at position N116 in p27 of the respiratory syncytial virus fusion protein elicits enhanced antibody responses after DNA immunization. Viruses 2018;10:E426. https://doi.org/10.3390/v10080426.

[17] McLellan JS, Yang Y, Graham BS, Kwong PD. Structure of respiratory syncytial virus fusion glycoprotein in the postfusion conformation reveals preservation of neutralizing epitopes. J Virol 2011;85:7788–96. https://doi.org/10.1128/JVI.00555-11.

[18] Arbiza J, Taylor G, López JA, Furze J, Wyld S, Whyte P, et al. Characterization of two antigenic sites recognized by neutralizing monoclonal antibodies directed against the fusion glycoprotein of human respiratory syncytial virus. J Gen Virol 1992;73(Pt 9):2225–34. https://doi.org/10.1099/0022-1317-73-9-2225.

[19] McLellan JS, Chen M, Kim A, Yang Y, Graham BS, Kwong PD. Structural basis of respiratory syncytial virus neutralization by motavizumab. Nat Struct Mol Biol 2010;17:248–50. https://doi.org/10.1038/nsmb.1723.

[20] Mousa JJ et al. Structural basis for nonneutralizing antibody competition at antigenic site II of the respiratory syncytial virus fusion protein. Proc Natl Acad Sci USA 2016;113:E6849–58. https://doi.org/10.1073/pnas.1609449113.

[21] McLellan JS, Chen M, Chang JS, Yang Y, Kim A, Graham BS, et al. Structure of a major antigenic site on the respiratory syncytial virus fusion glycoprotein in complex with neutralizing antibody 101F. J Virol 2010;84:12236–44. https://doi.org/10.1128/JVI.01579-10.

[22] Patel NFD, Lu H, Guebre-Xabier M, Zhou B, Smith G, Glenn G. RSV F nanoparticle immune responses target pre-fusion and post-fusion epitopes that together contribute to broadly neutralizing antibodies that are protective against live virus challenge. In: Presented at: RSV vaccines for the world (RSVVW) conference; November 29–December 1, 2017. Malaga, Spain.

[23] McLellan JS. Neutralizing epitopes on the respiratory syncytial virus fusion glycoprotein. Curr Opin Virol 2015;11:70–5. https://doi.org/10.1016/j.coviro.2015.03.002.

[24] Swanson KA, Settembre EC, Shaw CA, Dey AK, Rappuoli R, Mandl CW, et al. Structural basis for immunization with postfusion respiratory syncytial virus fusion F glycoprotein (RSV F) to elicit high neutralizing antibody titers. Proc Natl Acad Sci USA 2011;108:9619–24. https://doi.org/10.1073/pnas.1106536108.

[25] Kwakkenbos MJ, Diehl SA, Yasuda E, Bakker AQ, van Geelen CM, Lukens MV, et al. Generation of stable monoclonal antibody-producing B cell receptor-positive human memory B cells by genetic programming. Nat Med 2010;16:123–8. https://doi.org/10.1038/nm.2071.

[26] McLellan JS, Ray WC, Peeples ME. Structure and function of respiratory syncytial virus surface glycoproteins. Curr Top Microbiol Immunol 2013;372:83–104. https://doi.org/10.1007/978-3-642-38919-1_4.

[27] Zhao M, Zheng ZZ, Chen M, Modjarrad K, Zhang W, Zhan LT, et al. Discovery of a prefusion respiratory syncytial virus F-specific monoclonal antibody that provides greater in vivo protection than the murine precursor of palivizumab. J Virol 2017;91:e00176-17. https://doi.org/10.1128/JVI.00176-17.

[28] Mousa JJ, Kose N, Matta P, Gilchuk P, Crowe Jr JE. A novel pre-fusion conformation specific neutralizing epitope on the respiratory syncytial virus fusion protein. Nat Microbiol 2017;2:16271. https://doi.org/10.1038/nmicrobiol.2016.271.

[29] Smith G, Raghunandan R, Wu Y, Liu Y, Massare M, Nathan M, et al. Respiratory syncytial virus fusion glycoprotein expressed in insect cells form protein nanoparticles that induce protective immunity in cotton rats. PLoS ONE 2012;7:e50852. https://doi.org/10.1371/journal.pone.0050852.

[30] Glenn GM, Smith G, Fries L, Raghunandan R, Lu H, Zhou B, et al. Safety and immunogenicity of a Sf9 insect cell-derived respiratory syncytial virus fusion protein nanoparticle vaccine. Vaccine 2013;31:524–32. https://doi.org/10.1016/j.vaccine.2012.11.009.

[31] Glenn GM, Fries LF, Thomas DN, Smith G, Kpamegan E, Lu H, et al. A randomized, blinded, controlled, dose-ranging study of a respiratory syncytial virus recombinant fusion (F) nanoparticle vaccine in healthy women of childbearing age. J Infect Dis 2016;213:411–22. https://doi.org/10.1093/infdis/jiv406.

[32] August A, Glenn GM, Kpamegan E, Hickman SP, Jani D, Lu H, et al. A phase 2 randomized, observer-blind, placebo-controlled, dose-ranging trial of aluminum-adjuvanted respiratory syncytial virus F particle vaccine formulations in healthy women of childbearing age. Vaccine 2017;35:3749–59. https://doi.org/10.1016/j.vaccine.2017.05.045.

[33] Fries L, Shinde V, Stoddard JJ, Thomas DN, Kpamegan E, Lu H, et al. Immunogenicity and safety of a respiratory syncytial virus fusion protein (RSV F) nanoparticle vaccine in older adults. Immun Ageing 2017;14:8. https://doi.org/10.1186/s12979-017-0090-7.

[34] Raghunandan R, Lu H, Zhou B, Xabier MG, Massare MJ, Flyer DC, et al. An insect cell derived respiratory syncytial virus (RSV) F nanoparticle vaccine induces antigenic site II antibodies and protects against RSV challenge in cotton rats by active and passive immunization. Vaccine 2014;32:6485–92. https://doi.org/10.1016/j.vaccine.2014.09.030.

[35] Mejías A, Ramilo O. Review of palivizumab in the prophylaxis of respiratory syncytial virus (RSV) in high-risk infants. Biologics 2008;2:433–9.

[36] Turner TL, Kopp BT, Paul G, Landgrave LC, Hayes Jr D, Thompson R. Respiratory syncytial virus: current and emerging treatment options. Clin Outcom Res 2014;6:217–25. https://doi.org/10.2147/CEOR.S60710.

[37] Walsh EE, Wang L, Falsey AR, Qiu X, Corbett A, Holden-Wiltse J, et al. Virus-specific antibody, viral load, and disease severity in respiratory syncytial virus infection. J Infect Dis 2018;218:208–17. https://doi.org/10.1093/infdis/jiy106.

[38] Krarup A, Truan D, Furmanova-Hollenstein P, Bogaert L, Bouchier P, Bisschop IJ, et al. A highly stable prefusion RSV F vaccine derived from structural analysis of the fusion mechanism. Nat Commun 2015;6:8143. https://doi.org/10.1038/ncomms9143.

[39] Rossey I, Gilman MS, Kabeche SC, Sedeyn K, Wrapp D, Kanekiyo M, et al. Potent single-domain antibodies that arrest respiratory syncytial virus fusion protein in its prefusion state. Nat Commun 2017;8:14158. https://doi.org/10.1038/ncomms14158.

[40] Morton CJ, Cameron R, Lawrence LJ, Lin B, Lowe M, Luttick A, et al. Structural characterization of respiratory syncytial virus fusion inhibitor escape mutants: homology model of the F protein and a syncytium formation assay. Virology 2003;311:275–88. https://doi.org/10.1016/S0042-6822(03)00115-6.

[41] Gilbert BE, Patel N, Hanxin L, Ye L, Guebre-Xabier M, Piedra PA, et al. Respiratory syncytial virus fusion nanoparticle vaccine immune responses target multiple neutralizing epitopes that contribute to protection against wild-type and palivizumab-resistant mutant virus challenge. Vaccine 2018;36:8069–78. https://doi.org/10.1016/j.vaccine.2018.10.073.

[42] Gilman MS, Furmanova-Hollenstein P, Pascual G, van't Wout AB, Langedijk JP, McLellan JS. Transient opening of trimeric prefusion RSV F proteins. Nat Commun 2019;10:2105. https://doi.org/10.1038/s41467-019-09807-5.